

Supplementary Information

Dynamic self-assembly of charged colloidal strings and walls in simple fluid flows

Yu Abe,^{a,b} Bo Zhang,^a Leonardo Gordillo,^a Alireza Mohammad Karim,^a Lorraine F. Francis,^a and Xiang Cheng^a

^aDepartment of Chemical Engineering and Materials Science, University of Minnesota, Minneapolis, MN 55455, USA

^bFilm Products Research Laboratories, Toray Industries, Inc. 1-1, Sonoyama 1-chome, Otsu, Shiga, 520-8558, Japan

String structure at different heights

Colloidal strings can be observed next to the glass bottom (Fig. 2). However, the string structure is absent in the middle of the channel away from the glass bottom (Fig. S1a). Colloidal strings can also be observed next to the top boundary (Fig. S1b). The observation confirms that the gravity-induced sedimentation or flotation does not play a role in the formation of strings.

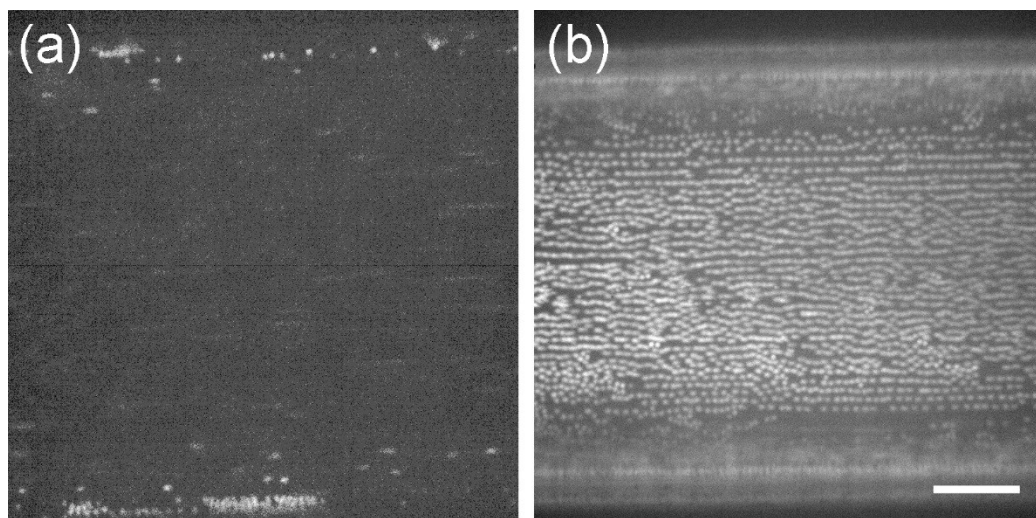


Fig. S1 Colloidal strings at different heights. (a) String structure is absent away from the glass bottom. The height is $z = 5 \mu\text{m}$ (b) Strings next to the top plate. Although particle concentration is fixed at 1%, more particles are attracted to the top PDMS surface than to the bottom glass surface (see Fig. 2). Flow rate is at $3.0 \mu\text{L}/\text{min}$. The scale bar is $20 \mu\text{m}$.

Spacing between strings

The spacings between strings show large variations. The average distance between strings decreases with increasing particle concentrations (Fig. S2).

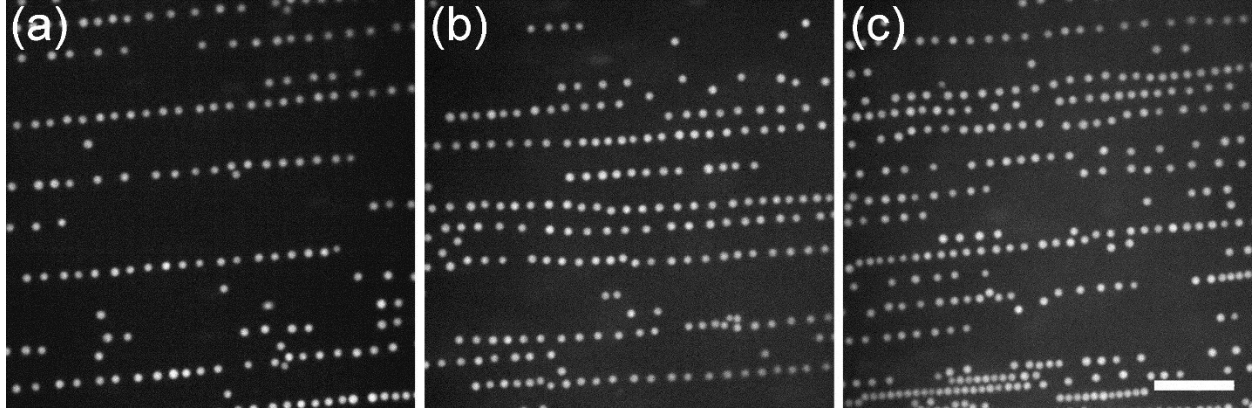


Fig. S2 String structures at different particle concentrations. (a) 0.25 wt%, (b) 0.5 wt% and (c) 1.0 wt%. The wide channel of $300 \times 100 \mu\text{m}^2$ was used. The flow rate is $9.0 \mu\text{L}/\text{min}$. The scale bar is $20 \mu\text{m}$.

Experimental errors related to the size of particles

(1) Errors on v_f

Experimentally, we determined the position of the center of a particle by adjusting the focal plane of the microscopic lens until the diameter of the particle under study appears to be maximal and the particle is in clear focus in the image. The z position of the microscopic lens can be controlled with a very high accuracy of $0.025 \mu\text{m}$ by using a lens piezo. Thus, the error in z mainly arises from the determination of the size of particles, d . To accurately determine the size of a colloidal particle is notoriously difficult (see the well-written review paper by Poon, Weeks & Royall, *Soft Matter* 2012). We determined the diameter of the particle from the position where the light-intensity profile of the particle first reaches the background intensity (Fig. S3 below). The diameter of the particle thus measured is close to the four standard deviations of the Gaussian fit of the intensity profile of the particle. In other words, the radius of the particle is about two standard deviations away from the center of the particle. The diameter of particles has an error about 1.5 pixels from our measurements, which leads to an absolute error of $\Delta d = \pm 0.049 \mu\text{m}$ and a relative error of $\Delta d/d \approx 3.5\%$, consistent with the literature values.⁴⁷ Alternatively, if the diameter of the particle is determined from the standard deviation of the Gaussian fit, the fitting error gives a similar relative error of $\Delta d/d \approx 3\%$. The uncertainty on particle sizes indeed gives rise to a relatively large error in the velocity of ambient flows due to the existence of high shear rates close to the boundary. Assuming the mean diameter of particles at $1.36 \mu\text{m}$, the channel cross-section at $100 \times 100 \mu\text{m}^2$ and the flow rate at $Q = 3 \mu\text{L}/\text{min}$ —the typical parameters of our experiments—the variation of particle diameter $\Delta d = \pm 0.049 \mu\text{m}$ leads to a relative error in ambient flow velocities of $\Delta v_f/v_f \sim 7\%$ near the center of the channel next to the glass bottom. The difference between velocities at different z will be smaller when the particle is close to the side wall at $y = \pm 50 \mu\text{m}$. This relatively large error of $\Delta v_f/v_f$ contributes, in a large part, to the scattering of data in Fig. 4. Nevertheless, this error is still significantly smaller than the range of velocity differences between particles and the ambient flow, $(v_f - v_p)/v_f$, we measured in our experiments. As such, the

uncertainty should not qualitatively change our conclusions, i.e., the existence of finite velocity differences between particles and the ambient flow.

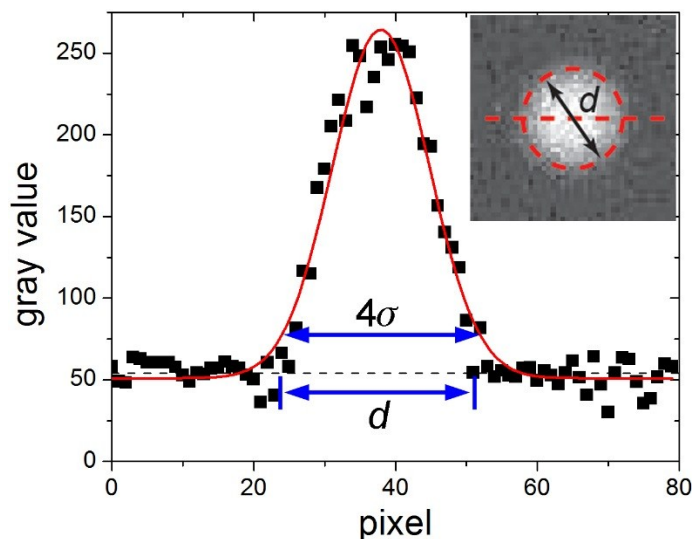


Fig. S3 The light-intensity profile of a particle from confocal microscopy. The intensity is measured through the center of the particle along the horizontal dashed line (see inset). The center of the particle is obtained via a widely-used particle tracking algorithm,³⁴ where a 2D Gaussian fit of the particle image is used to achieve a subpixel resolution. The horizontal black dashed line indicates the background intensity measured far away from the particle. The diameter of the particle, d , is then measured from the positions where the particle intensity first reaches the background intensity as indicated in the plot. The solid red line is a Gaussian fit of the profile. σ is the standard deviation of the Gaussian fit. 4σ is indicated in the plot.

(2) Errors on a_2/a_1

Although the error on the size of one single particle is large, the relative error on the size ratio of two particles is small.⁴⁷ To determine the size ratio a_2/a_1 , we fit the intensity profiles of the two particles with two independent Gaussian distributions. Assuming the size of particles in the focal plane is proportional to the standard deviation of the Gaussian distributions, we have $r_1 = c \cdot \sigma_1$ and $r_2 = c \cdot \sigma_2$, where c is an unknown constant, σ_1 and σ_2 are the standard deviations of the two Gaussian fits. Since the focal plane is chosen to be through the largest circle of the small particle, $a_1 = r_1 = c \cdot \sigma_1$ (see Fig. 2 below). The radius of the large particle, Particle 2, can then be calculated through a simple geometry (Fig. 2), giving $a_2 = (r_2^2 + a_1^2)/(2a_1) = c(\sigma_1^2 + \sigma_2^2)/(2\sigma_1)$. Hence, the ratio $a_2/a_1 = (\sigma_1^2 + \sigma_2^2)/(2\sigma_1^2)$. The error of a_2/a_1 is then given by

$$\Delta(a_2/a_1) = \sqrt{\frac{\sigma_2^4}{\sigma_1^6}(\Delta\sigma_1)^2 + \frac{\sigma_2^2}{\sigma_1^4}(\Delta\sigma_2)^2}$$

where $\Delta\sigma_1$ and $\Delta\sigma_2$ are the fitting errors of the Gaussian distributions. Since the measurements on the size of the two particles are independent, we should have $\sigma_1 \approx \sigma_2$ and $\Delta\sigma_1 \approx \Delta\sigma_2$. Thus, we have $\Delta(a_2/a_1) = \sqrt{2}(\Delta\sigma_1/\sigma_1)$. From a typical fitting result (see e.g. Fig. S3), we estimate $\Delta(a_2/a_1) \approx 4.1\%$.

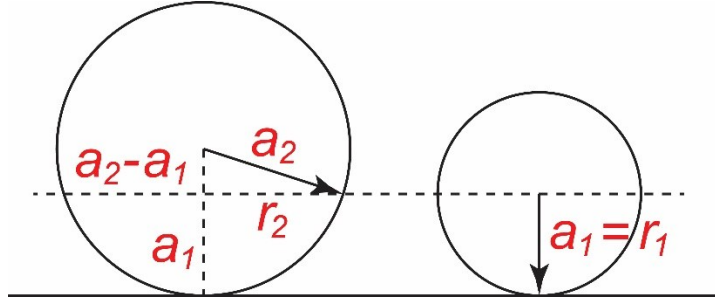


Fig. S4 A schematic showing the calculation of the size ratio of two particles, a_2/a_1 .

Comparison between the calculated and measured velocity profiles

We measured the velocity profiles with tracer particles at two different heights above the bottom plate in a wide channel. The calculated velocity profiles agree with the measured velocity profiles (Fig. S5), which directly validates our calculation.

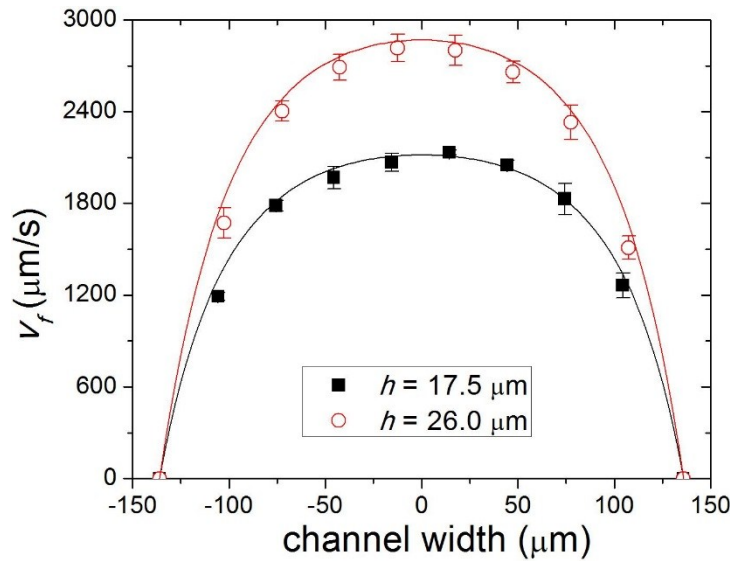


Fig. S5 Comparison of calculated velocity profiles (solid lines) and measured velocity profiles (symbols). The channel has a cross-section area of $272 \times 114 \mu\text{m}^2$. The flow rate is $4 \mu\text{L}/\text{min}$. h is the height above the bottom plate.

Additional references:

47. W. C. K. Poon, E. R. Weeks and C. P. Royall, *Soft Matter*, 2012, **8**, 21-30.